Electronic and thermoelectric properties of $Mg_2Ge_xSn_{1-x}$ ($x = 0.25, 0.50, 0.75$) solid solutions by first-principles calculations

Kai-yue Li(李开跃), Yong Lu(鲁勇)[†], Yan Huang(黄艳), and Xiao-hong Shao(邵晓红)[‡]

College of Science, Beijing University of Chemical Technology, Beijing 100029, *China*

(Received 18 January 2017; revised manuscript received 4 March 2017; published online 20 April 2017)

The electronic structure and thermoelectric (TE) properties of $Mg_2Ge_xSn_{1-x}$ ($x = 0.25$, 0.50, 0.75) solid solutions are investigated by first-principles calculations and semi-classical Boltzmann theory. The special quasi-random structure (SQS) is used to model the solid solutions, which can produce reasonable band gaps with respect to experimental results. The n-type solid solutions have an excellent thermoelectric performance with maximum zT values exceeding 2.0, where the combination of low lattice thermal conductivity and high power factor (PF) plays an important role. These values are higher than those of pure Mg_2Sn and Mg_2Ge. The p-type solid solutions are inferior to the n-type ones, mainly due to the much lower PF. The maximum zT value of 0.62 is predicted for p-type $Mg_2Ge_{0.25}Sn_{0.75}$ at 800 K. The results suggest that the n-type $Mg_2Ge_xSn_{1-x}$ solid solutions are promising mid-temperature TE materials.

Keywords: solid solution, electronic structure, thermoelectric transport property

PACS: 61.50.–f, 74.25.fc **DOI:** 10.1088/1674-1056/26/6/066103

1. Introduction

Thermoelectric (TE) materials have attracted lots of attention because of their wide application prospects in the recovery of waste heat, the efficiency of which are measured by the dimensionless figure of merit, $zT = \sigma S^2 T/(\kappa_e + \kappa_l)$, where S, T, σ, and $(\kappa_e + \kappa_l)$ are the Seebeck coefficient, temperature, electrical conductivity, and thermal conductivity contributed by electron (κ_e) and lattice (κ_l), respectively. For promising commercial TE materials, they should have high zT combining simultaneously high power factor $S^2\sigma$ and low thermal conductivity. Materials with $zT > 1$, such as PbTe-based alloys,[1] layered SnSe,[2] BiCuSnO oxyselenides,[3–5] Skutterudites,[6,7] half-Heusler MgAgSb,[8,9] copper chalcogenides,[10] graphdiyne,[11] and Mg_2Si-based solid solutions,[12–20] have been considered for large-scale power generation application at the mid-temperature region between 400 K and 800 K. Although developing higher zT value TE materials has always been the core issue, ensuring environmental friendliness is also becoming more and more important.

The solid solution Mg_2X (X = Si, Ge, Sn) compounds are made from naturally abundant non-toxic elements, which are promising green TE materials. Compared to PbTe-based TE materials, Mg_2X compounds have the innate advantages of being non-toxic and low density. Most studies have been focused on the TE performance of Mg_2X system, where the zT of n-type is significantly higher than that of the p-type.[19] The inferior p-type performance is mainly due to the much lower intrinsic hole mobility with respect to electron mobility in Mg_2X compounds.[21] In pure binary Mg_2X compounds, Mg_2Sn has the highest hole to electron mobility ratio, which is considered as the appropriate test bed for p-type doping. Moreover, it is found that the intrinsic thermal conductivity is high for any pure binary Mg_2X, thus, it is hard to achieve a high zT without introducing strong phonon scattering, such as solid solution and impurity doping, etc. Many efforts have been made to investigate the TE performance of Mg_2X solid solution system. For instance, Liu *et al.*[13] studied the n-type $Mg_2Si_{1-x}Sn_x$ solid solutions and found a zT value of 1.3 at 700 K; Liu *et al.*[22] studied the TE properties of n-type $Mg_2Ge_{0.25}Sn_{0.75}$, where the zT value reached 1.4 at 723 K; Jiang *et al.*[23] have successfully synthesized a p-type $Mg_{1.98}Ge_{0.4}Sn_{0.6}Ag_{0.02}$ with zT value of 0.38 at 675 K; Boor *et al.*[24] investigated the potential of p-type $Mg_2Ge_{0.4}Sn_{0.6}$ using Li as dopant, predicting a high power factor of 1.7×10^{-3} W/mK^2 at 700 K and $zT_{max} > 0.5$; Sun *et al.*[19] researched $Mg_2Ge_{0.5}Sn_{0.5}$ solid solution using supercell models based on first-principles calculations and found a peak zT value of 2.25 for n-type and 0.4 for p-type at 1000 K. Theoretically, the simple approach based on first principles calculations to model solid solution compounds is the supercell method. However, due to the limitations of computer performance, the conventional size of the first principles supercell can only be hundreds of atoms, which is far from enough to restore a real disordered state. Therefore, several methods have been proposed to deal with this problem, such as the cluster

*Project supported by the National Natural Science Foundation of China (Grant No. 11647010) and the Foundation from the Higher Education and High-quality and World-class Universities (Grant No. PY201611).

†Corresponding author. E-mail: luy@mail.buct.edu.cn

‡Corresponding author. E-mail: shaoxh@mail.buct.edu.cn

© 2017 Chinese Physical Society and IOP Publishing Ltd

expansion,[25] special quasi-random structure (SQS),[26] and the virtual crystal structure method.[27] Among them, the SQS method has been successfully combined with first principles to study the electronic and thermodynamic properties of disordered phases,[28–30] the basic idea of which is to produce an SQS with configurational correlation functions (CF) very close to those of solid solutions.

In this study, we investigate the TE properties of n-type and p-type $Mg_2Ge_xSn_{1-x}$ ($x = 0.25$, 0.50, 0.75) solid solutions based on first-principles and SQS method. Mg_2(Ge, Sn) solid solutions have been pointed out to having a favorable hole to electron mobility ratio, which are considered to be the most promising for p-type thermoelectricity.[31,32] Balancing the limitation of computer capability and calculation accuracy, we take the maximum usage of SQS-24 cell to model the disorder phase. We obtained higher zT values for both n-type and p-type $Mg_2Ge_xSn_{1-x}$ compared with the ordered supercell due to the fact that SQS structures are closer to the real disordered state with respect to the traditional supercell method. Further comparison with literature data provides some understanding of the influence of the Ge/Sn ratio on electronic and TE properties.

2. Computational detail

In this study, we consider mixing the anion sublattice of the rocksalt crystal structure $Mg_2Ge_xSn_{1-x}$ with $x =$ 0.25, 0.5, and 0.75. The SQSs were generated by using the ATAT package.[33] These structural relaxations and energetic calculations were performed using density functional theory (DFT) as implemented in Vienna *Ab-initio* Simulation Package (VASP).[34] The electron–ion interaction is described by the projector-augmented-wave (PAW) method.[35] The generalized-gradient approximation (GGA) with Perdew, Burke, and Ernzerhof (PBE) form[36] is used to describe the exchange–correlation function. The plane-wave cutoff energy is 450 eV, and the energy convergence criterion is chosen to be 10^{-5} eV. The integration over the Brillouin zone (BZ) is done with $5 \times 5 \times 5$ Monkhorst–Pack grid meshes[37] to ensure the Hellmann–Feynman forces on each ion to be less than 0.05 eV $\cdot$ Å^{-1} and energy converged to less than 0.1 meV. Phonon dispersion curves of SQSs were calculated using $2 \times 2 \times 2$ supercell by the density functional perturbation theory (DFPT) with the help of Phonopy package.[38]

The TE transport properties of $Mg_2Ge_xSn_{1-x}$ were calculated by the linearized augmented-plane-wave (LAPW) method using the WIEN2k code.[39] The cutoff parameter for the basis is $R_{\min}K_{\max} = 7$, and the number of k points is 1000 in BZ for the self-consistent calculations. The modified Becke–Johnson potential of Tran and Blaha (TB-mBJ)[40,41] is used to obtain the electronic structures. The TE transport properties were calculated through the semi-classical Boltzmann theory and the rigid-band approach as implemented in the BoltzTraP code.[42] The constant scattering time approximation (CSTA) is used, which is based on the assumption that the scattering time determining the electrical conductivity does not vary strongly with energy on the scale of k_BT. This approximation does not involve any assumption about the possible strong doping and temperature dependence of relaxation time, τ, which has been successfully applied in predicting electrical transport properties for many TE materials.[43–45] In this way, the Seebeck coefficient S is independent of τ, while the electrical conductivity σ and κ_e can only be evaluated with respect to the parameter τ.

3. Results and discussion

3.1. Atomic structure and phase stability

In order to produce the fraction $x = 0.25$ and 0.75, the minimum SQS supercell should contain 12 atoms. In this study, we consider mixing on the anion sublattice of the rocksalt crystal structure. For each fraction, the atom positions are randomly exchanged between the atoms, terminated until the atomic arrangement of a supercell converges to the closest CFs of the random solution and the error is estimated by $\Sigma(\Pi_{k,m}^{\text{ideal}} - \Pi_{k,m})^2$. The CFs of pairs and triplets are listed in Table 1.

Table 1. Pair and multi-site correlation functions of SQS structures for $Mg_2Ge_xSn_{1-x}$ solid solutions.

	$x = 0.25$			$x = 0.5$			$x = 0.75$		
Figure	Random	SQS-12	SQS-24	Random	SQS-12	SQS-24	Random	SQS-12	SQS-24
$\Pi_{2,1}$[06]	0.25	–0.0833	0.1667	0	0	0	0.25	–0.0833	0.1667
$\Pi_{2,2}$[03]	0.25	–0.25	0.1667	0	–0.3333	0	0.25	–0.25	0.1667
$\Pi_{2,3}$[12]	0.25	0	0.25	0	0	–0.1667	0.25	0	0.25
$\Pi_{2,4}$[06]	0.25	0.25	0.1667	0	–0.3333	0.3333	0.25	0.25	0.1667
$\Pi_{2,5}$[12]	0.25	0.0833	0.3333	0	0	0	0.25	0.0833	0.3333
$\Pi_{2,6}$[04]	0.25	–0.25	0.375	0	1	0	0.25	–0.25	0.375
$\Pi_{2,7}$[24]	0.25	0	0.2917	0	0	–0.1667	0.25	0	0.2917
$\Pi_{3,1}$[08]	0.125	–0.125	0	0	0	0	0.125	–0.125	0
$\Pi_{3,2}$[12]	0.125	–0.2917	0	0	0	0	0.125	–0.2917	0
Error	0	1.0	0.0764	0	1.2222	0.1667	0	1.0	0.0764

For the SQS-12 supercell, the errors of the CF are 1.0 for $x = 0.25$ (0.75) and 1.22 for $x = 0.5$ accounting for the 7th nearest neighbors. Though SQS-12 possesses many pair correlations that match the random alloy statistics, the discrepancies are relatively large. In order to minimize error, we doubled the SQS supercell, and the CFs of SQS-24 are also listed in Table 1. Compared to SQS-12, the usage of SQS-24 supercell reduces the error largely with more pair correlations matching the random alloy statistics for all these three proportions. For $x = 0.25$ (0.75), the error of the 7th nearest neighbors is only 0.0764. Although enlarging the SQS supercell may further reduce the error, this size represents a good compromise between accuracy and the computational requirements associated with the TE transport property calculations. Thus, in the following, we choose the SQS-24 for the electronic and TE property studies.

The special quasi-random structures with 24 atoms for these three solid solutions are shown in the following Fig. 1. The optimized lattice constants are $a = 8.23$ Å, $b = 8.24$ Å, $c = 9.51$ Å for $Mg_2Ge_{0.25}Sn_{0.75}$, $a = 5.47$ Å, $b = 9.61$ Å, $c = 11.49$ Å for $Mg_2Ge_{0.5}Sn_{0.5}$, and $a = 8.23$ Å, $b = 8.24$ Å, $c = 9.51$ Å for $Mg_2Ge_{0.75}Sn_{0.25}$, respectively. Correspondingly, the volume of $Mg_2Ge_{0.25}Sn_{0.75}$ is 608.79 Å^3, which is slightly larger than that of 580.89 Å^3 for $Mg_2Ge_{0.5}Sn_{0.5}$ and 556.80 Å^3 for $Mg_2Ge_{0.75}Sn_{0.25}$.

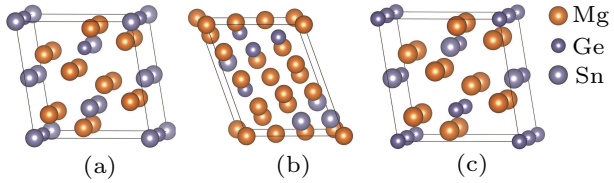


Fig. 1. (color online) The SQSs of $Mg_2Ge_xSn_{1-x}$ solid solutions with (a) x=0.25, (b) x=0.5, and (c) x=0.75, respectively. The number of atoms in the SQS unit cell is 24.

Using these SQSs, we calculated the phonon dispersion curves, as shown in Fig. 2, in comparison with the counterparts of pure Mg_2Ge and Mg_2Sn. Clearly, there are no imaginary frequencies existing in all these phonon dispersion relations, indicating the dynamical stability of these SQSs. Compared to the pure Mg_2Sn and Mg_2Ge, the slopes of acoustic modes of solid solutions are reduced largely, reflecting a lower phonon group velocity. The low-frequency optical modes are mixed with the acoustic branches in $Mg_2Ge_{0.5}Sn_{0.5}$ and $Mg_2Ge_{0.75}Sn_{0.25}$, showing the strong phonon scattering between them. Both the low group velocity and strong phonon scattering are beneficial to reducing the lattice thermal conductivity.

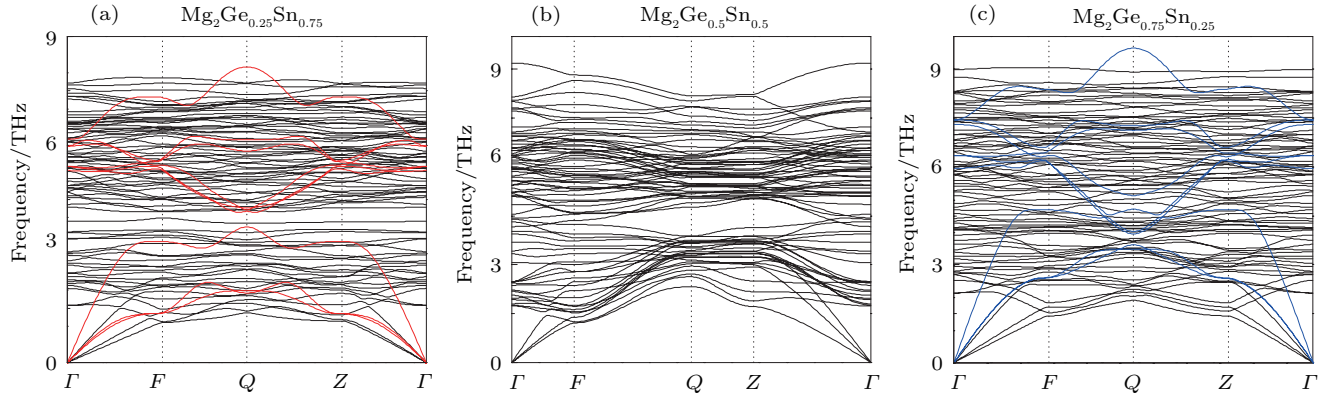


Fig. 2. (color online) The calculated phonon dispersion curves of $Mg_2Ge_xSn_{1-x}$ at (a) x=0.25, (b) x=0.5, and (c) x=0.75, respectively. The corresponding results of Mg_2Sn (red solid lines in panel (a)) and Mg_2Ge (blue solid lines in panel (c)) are also shown for comparison.

3.2. Electronic structure

The total density of states (DOS) and projected density of states of $Mg_2Ge_xSn_{1-x}$ solid solutions are shown in Fig. 3, compared with those of pure Mg_2Sn and Mg_2Ge. In general, all these densities of states are featured by four well-resolved peaks, distributed on both sides of Fermi level. From Fig. 3(a), the slope of the total DOS at VBM is larger than that of CBM for any compositions, indicating that the effective mass of carriers of p-type is larger than that of n-type. Since the effective mass is proportional to the Seebeck coefficient (S), the value of S for p-type $Mg_2Ge_xSn_{1-x}$ is also larger than that of n-type. From the partial density of states (PDOS) as shown in Figs. 3(b)–3(f), the peak at CBM is largely observed by the Mg-s orbital, while the peak at VBM nearby is mainly contributed by the Sn-p orbital for $Mg_2Ge_{25}Sn_{0.75}$ and Ge-p orbital for $Mg_2Ge_{0.75}Sn_{0.25}$ respectively, indicating the occurrence of charge transfers from Mg to Sn or Ge. Through the Bader analysis,[46] we can obtain the charge transfer quantitatively, where about two electrons are transferred from Mg atom to Sn atom in $Mg_2Ge_{0.25}Sn_{0.75}$ or to Ge atom in $Mg_2Ge_{0.75}Sn_{0.25}$. In $Mg_2Ge_{0.5}Sn_{0.5}$, the Sn and Ge atoms are almost equivalent in sharing the electrons. Further analysis shows that these electrons are mainly from the Mg-3s orbital. As x increases from 0.25 to 0.75, the band gap between VBM and CBM is enlarged from 0.35 eV to 0.44 eV. These values lie in the experimental results for the pure Mg_2Sn of 0.3 eV and Mg_2Ge of 0.6 eV.[47] It is noted that the band gap of $Mg_2Ge_{0.5}Sn_{0.5}$ calculated by the ordered supercell is 0.23 eV,[19] which is slightly lower than that of the pure Mg_2Sn and the present result of 0.4 eV.

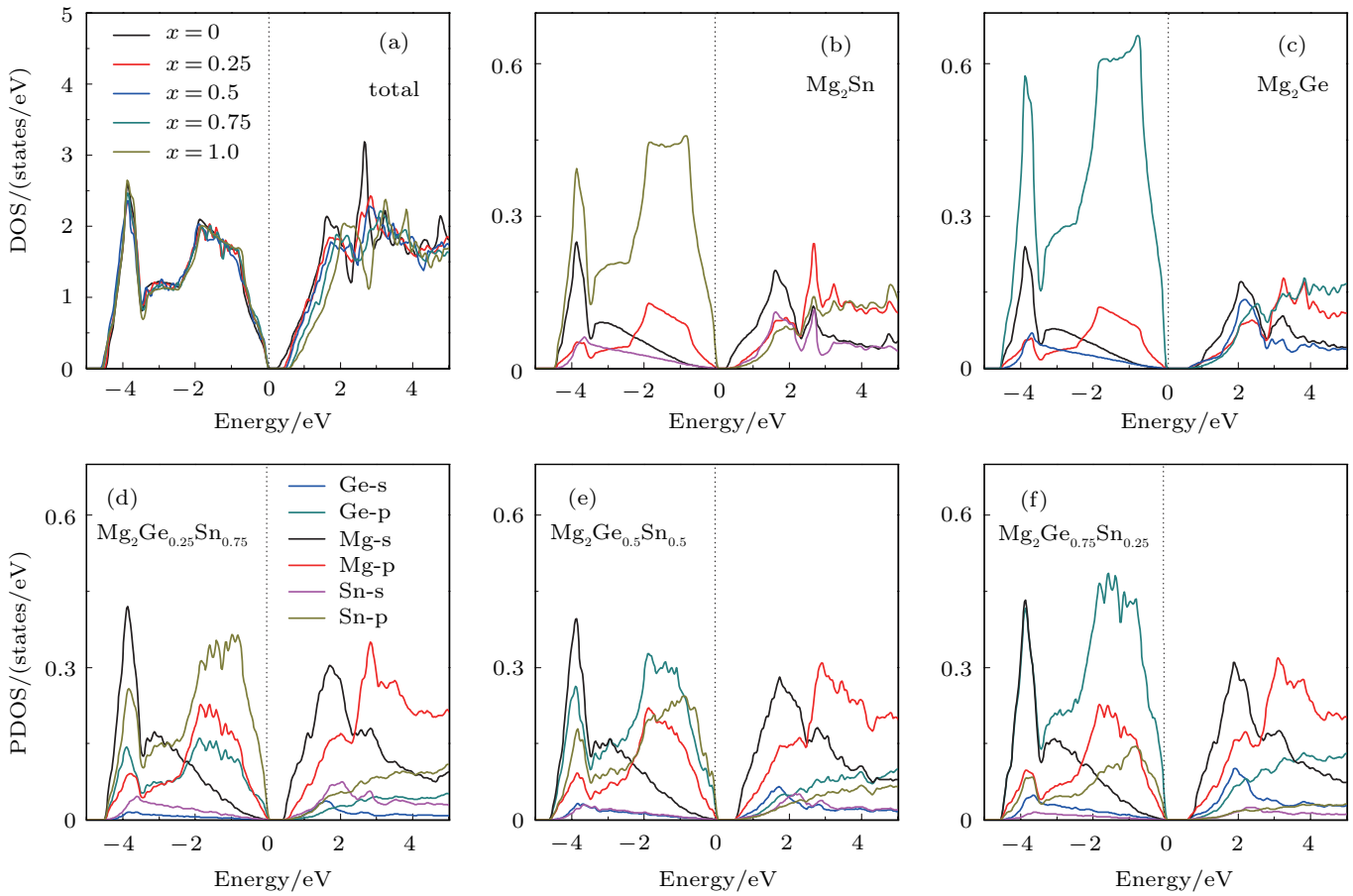


Fig. 3. (color online) (a) shows the total DOS for $Mg_2Ge_xSn_{1-x}$ at $x = 0$, 0.25, 0.5, 0.75, 1. Panels (b)–(f) show the projected DOS of $Mg_2Ge_xSn_{1-x}$ solid solutions. All the Fermi levels have been set at zero.

3.3. Debye temperature and lattice thermal conductivity

The Debye temperature (Θ_D) describes atomic vibrations to be elastic waves and it is related to the sound velocity.[48] The Debye temperature can be expressed as follows:

$$\Theta_D = \frac{h}{k_B}\left(\frac{3n}{4\pi\Omega}\right)^{1/3} v_m, \quad (1)$$

where h and k_B are Planck and Boltzmann constants, respectively, n is the number of atoms in one unit cell, Ω is the volume per unit cell, and v_m is the averaged sound velocity. Approximately, the averaged sound velocity can be calculated by the following expression

$$v_m = \left[\frac{1}{3}\left(\frac{2}{v_t^3} + \frac{1}{v_l^3}\right)\right]^{-1/3}, \quad (2)$$

where $v_t = \sqrt{G/\rho}$ is the transverse elastic wave velocity, (ρ is the density of a material) and $v_l = \sqrt{[B+(4/3)G]/\rho}$ is the longitudinal elastic wave velocity. B and G are the bulk and shear modulus, which can be determined by elastic constants following $B = (C_{11}+2C_{12})/3$ and $G = (C_{11}-C_{12}+3C_{44})/5$, respectively. The elastic constants C_{11} ,C_{12}, and C_{44} are obtained by enforcing small strains on the equilibrium unit cell based on Hooke's law.[49] Our calculated elastic moduli, sound velocities and Debye temperature of $Mg_2Ge_xSn_{1-x}$ are listed in Table 2. As x increases, the values of v_t and v_l show decrease trends. $Mg_2Ge_{0.25}Sn_{0.75}$ has the lowest Debye temperature due to the fact that Θ_D is proportional to v_m according to Eq. (1).

Table 2. The calculated elastic constants (C_{ij}, in unit GPa), bulk modulus (B, in unit GPa), shear modulus (G, in unit GPa), density (ρ, in units g/cm^3), volume (V, in units Å^3), transverse sound velocity (v_t, in units m/s), longitudinal sound velocity (v_l, in units m/s), mean sound velocity (v_m, in units m/s), Debye temperature (Θ_D, in unit K), and minimum lattice thermal conductivity (κ_{min}) of $Mg_2Ge_xSn_{1-x}$ ($x = 0.25$, 0.5, 0.75) solid solutions.

Phase	C_{11}/GPa	C_{12}/GPa	C_{44}/GPa	ρ/(g/cm^3)	V/Å^3	B/GPa	G/GPa	v_t/(m/s)	v_l/(m/s)	Θ_D/K	κ_{min}
$Mg_2Ge_{0.25}Sn_{0.75}$	83.87	22.04	28.34	3.41	25.38	42.65	29.37	2935	4898	329	0.69
$Mg_2Ge_{0.5}Sn_{0.5}$	90.02	22.10	31.80	3.30	24.27	44.74	32.66	3146	5173	358	0.76
$Mg_2Ge_{0.75}Sn_{0.25}$	90.42	22.43	32.27	3.19	23.14	45.09	32.96	3214	5283	372	0.80

Based on Debye theory, the lattice thermal conductivity is proportional to $1/T$ at low temperature and reaches the minimum value at high temperature. When the temperature is higher than the Debye temperature, the lattice thermal conductivity can be well estimated using the minimum lattice thermal conductivity ($\kappa_{\min}$), where the phonon scattering is dominated by the Umklapp process. The $\kappa_{\min}$ can be calculated according to the following expression[50]

$$\kappa_{min} = \frac{1}{2}\left(\frac{\pi}{6}\right)^{1/3} k_B V^{-2/3}(2v_t + v_l), \tag{3}$$

with V the average volume per atom. The results are also listed in Table 2. Among these three solid solutions, $Mg_2Ge_{0.25}Sn_{0.75}$ has the lowest $\kappa_{\min}$ of 0.69 $W \cdot m^{-1} \cdot K^{-1}$, originating from its larger V and lower acoustic velocities. This value is somewhat lower than the experimental data of ~ 1.2 $W \cdot m^{-1} \cdot K^{-1}$ for $Mg_2Ge_{0.25}Sn_{0.75}$ at 723 K.[22] Since the minimum thermal conductivity should be regarded as the lower limit of the lattice thermal conductivity for solid solutions, it provides predictive theoretical guidance for methods to further reduce the lattice thermal conductivity, such as the fabrication and synthesis of nanostructures.[51]

3.4. Thermoelectric transport properties

The TE transport properties of $Mg_2Ge_xSn_{1-x}$ solid solutions were calculated by semi-classical Boltzmann theory with CSTA. Using the W–F formula, $\kappa_e = L\sigma T$, the zT can be further expressed as $zT = rS^2/L$, where $L = 2.45 \times 10^{-8}$ $W \cdot \Omega/K^2$ is the standard Lorenz number and $r = \kappa_e/(\kappa_e + \kappa_l) \leq 1$. Thus, in order to obtain the zT value, one still needs to calculate the σ and S parameters. It is well known that the carrier concentration of a TE material with a good performance is in the range of 10^{19} to 10^{20} carriers per cm^{-3}.

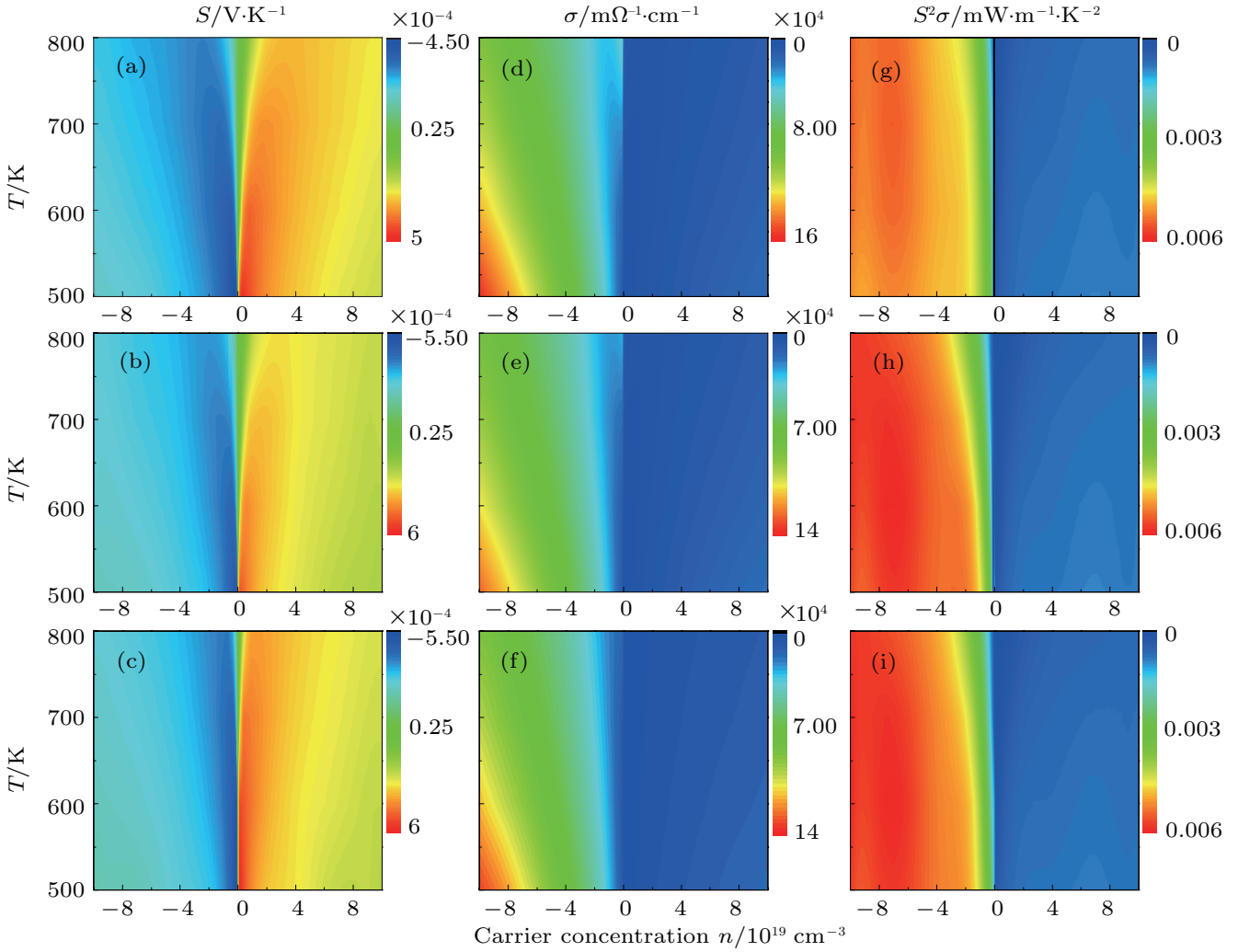


Fig. 4. (color online) Transport coefficients map of $Mg_2Ge_xSn_{1-x}$ as a function of carrier concentration n and temperature T for $x = 0.25$ (top), 0.50 (mid), 0.75 (bottom), respectively. Panels (a)–(c) show the Seebeck coefficient; panels (d)–(f) show the electronic conductivity; panels (g)–(i) show the power factor. The negative scale of x axis stands for the n-type, while the positive scale represents the p-type.

Thus, in Fig. 4, we show the calculated S as a function of carrier concentration at this range. According to the definition of Seebeck coefficient,

$$S = \frac{8\pi^2 k_B^2}{3eh^2} m^* T \left(\frac{\pi}{3n}\right)^{2/3}, \tag{4}$$

the S is proportional to the effective mass of carrier, m^*. From

Fig. 4, generally, the S of p-type $Mg_2Ge_xSn_{1-x}$ solid solutions is larger than that of n-type covering the whole range of concentrations considered here, consistent with the larger valence-band effective mass. We note that there is a flexion of the S curve in these solid solutions. As temperature increases, the absolute value of S decreases at low concentration but increases at high concentration. Actually, at high concentration, S increases with increasing temperature due to the proportionality between S and T. However, at low concentration, the bipolar effect[52] plays an important role in the contribution of S, which originates from the two types of carriers introduced by a small band gap. The dipolar effect limits the TE performance, which should be reduced as much as possible in applications. This character also appears in the pure Mg_2Sn material.[53]

From the electronic structures above, σ/τ can be easily calculated as a function of carrier concentration and temperature. However, in order to isolate the electrical conductivity σ, one should use the relation, $\sigma = (\sigma/\tau) \times \tau$, based on the CSTA, where the scattering time τ should be known. In typical electron–phonon regime, τ is proportional to $T^{-1}n^{-1/3}$. Thus, in the following, we use the experimental data to determine τ and obtain the electrical conductivity σ. For p-type $Mg_2Ge_xSn_{1-x}$ ($x = 0.25$, 0.5), the experimental data from Jiang *et al.*[23] is used. In this literature, the Ag-doped $Mg_{1.98}Ag_{0.02}Ge_{0.4}Sn_{0.6}$ solid solution has been successfully synthesized. We select the same typical temperature of 400 K as that in Ref. [19]. At 400 K, the Seebeck coefficient S is about 203 μV/K. Compared with the calculated S from Fig. 4(a), the corresponding carrier concentration is 9.4×10^{19} cm^{-3}. Using the experimental electrical conductivity of 2.00×10^4 S/m and the calculated σ/τ, we obtain a relaxation time of $\tau = 0.56 \times 10^{-5} T^{-1} n^{-1/3}$. For n-type, we choose the data from Liu *et al.*[22] at 300 K. Similarly, we obtain the $\tau = 3.9 \times 10^{-5} T^{-1} n^{-1/3}$. Due to the lack of experimental data for $Mg_2Ge_{0.75}Sn_{0.25}$, we adopt the same scattering time as that for $Mg_2Ge_{0.25}Sn_{0.75}$. The calculated electrical conductivities for these three types of solid solution are shown in Figs. 4(d)–4(f). Evidently, the σ of the n-type is several times higher than that of the p-type for all three solid solutions.

The corresponding power factors (PF), $S^2\sigma$, can then be obtained, which are shown in Figs. 4(g)–4(i). The general characteristics of these curves are similar with one peak at each temperature. With the increase of carrier concentration, the value of PF increases firstly to the maximum value and then decreases. This is because PF is mainly dominated by σ at low carrier concentrations, while S plays an important role in PF at high carrier concentrations. The maximum value of PF is 0.8 mW/mK^2 for p-type $Mg_2Ge_{0.25}Sn_{0.75}$ at 500 K and 5.96 mW/mK^2 for n-type $Mg_2Ge_{0.5}Sn_{0.5}$ at 700 K, which is in good agreement with the experimental data, i.e., 0.9 mW/mK^2 at 500 K for p-type $Mg_2Ge_{0.4}Sn_{0.6}$[23] and 5.4 mW/mK^2 for n-type $Mg_2Ge_{0.25}Sn_{0.75}$.[22]

We show in Fig. 5 the calculated electronic thermal conductivity, κ_e, as a function of carrier concentration from 10^{19} cm^{-3} to 10^{20} cm^{-3} and temperature from 500 K to 800 K, according to the Wiedemann–Franz relation, $\kappa_e = L\sigma T$. In general, the κ_e increases monotonically with increasing the carrier concentration for both p-type and n-type, similar to the results of σ. As the concentration increases from 10^{19} cm^{-3} to 10^{20} cm^{-3}, the κ_e of the n-type solid solutions is increased from ~ 0.2 W·m^{-1}·K^{-1} to ~ 2 W·m^{-1}·K^{-1}, in agreement with the experimental values from ~ 1.1 W·m^{-1}·K^{-1} to ~ 1.3 W·m^{-1}·K^{-1} for $Mg_2Ge_{0.25}Sn_{0.75}$ with temperature increasing from 298 K to 723 K.[22] The κ_e of the p-type is lower than that of the n-type by an order of magnitude, which is increased from ~ 0.05 W·m^{-1}·K^{-1} to ~ 0.2 W·m^{-1}·K^{-1} with the concentration increasing from 10^{19} cm^{-3} to 10^{20} cm^{-3}. The experimental κ_e for the p-type $Mg_2Ge_{0.5}Sn_{0.5}$ can be approximated by the difference between the κ and κ_l, which is increased from ~ 0.05 W·m^{-1}·K^{-1} to ~ 0.15 W·m^{-1}·K^{-1} with temperature increasing from 500 K to 700 K.[23] Our theoretical results are also consistent with these observations.[22,23] The total thermal conductivity can then be evaluated by the combination of κ_e and κ_l.

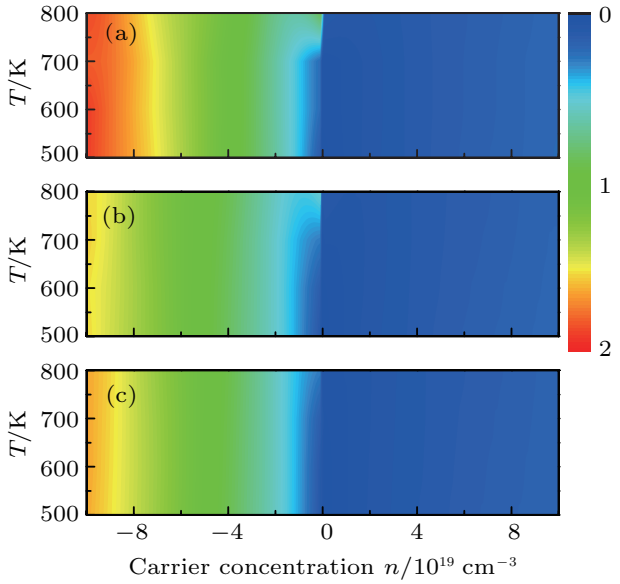


Fig. 5. (color online) Calculated κ_e of $Mg_2Ge_xSn_{1-x}$ with (a) $x = 0.25$, (b) $x = 0.5$, and (c) $x = 0.75$ as a function of the carrier concentration n and the temperature T, respectively. The negative scale of x axis stands for the n-type, while the positive scale represents the p-type.

All the TE parameters are unified by zT value to measure the TE performance. In Fig. 6, we show the calculated

zT values of $Mg_2Ge_xSn_{1-x}$ solid solution as a function of temperature from 500 K to 800 K and carrier concentration from 10^{19} cm^{-3} to 10^{20} cm^{-3}. It can be seen that the zT value of the n-type $Mg_2Ge_xSn_{1-x}$ is much higher than that of the p-type, which can be mainly attributed to the much higher PF for the n-type. The maximum of zT value reaches 2.45 for the n-type $Mg_2Ge_{0.5}Sn_{0.5}$ at 800 K with a carrier concentration of 3.28×10^{19} cm^{-3}, mainly due to combination of high PF and low lattice thermal conductivity. We note that this value is slightly higher than that of 2.25 for $Mg_2Ge_{0.5}Sn_{0.5}$ in Ref. [19], which is obtained by the ordered supercell method. Similarly, the $Mg_2Ge_{0.25}Sn_{0.75}$ and $Mg_2Ge_{0.75}Sn_{0.25}$ also show high TE performance with zT of 2.31 and 2.40, respectively. These results are higher than the experimental data of 1.4 for $Mg_2Ge_{0.25}Sn_{0.75}$ at a different carrier concentration of 3.0×10^{20} cm^{-3}. At the same concentration, we obtain a zT value of 0.9. The differences between the theoretical and experimental values may originate from the CSTA or temperature effects or a combination. The maximum zT value of 0.62 for the p-type $Mg_2Ge_xSn_{1-x}$ solid solution appears at $x = 0.25$, which is still about four times lower than that of the n-type.

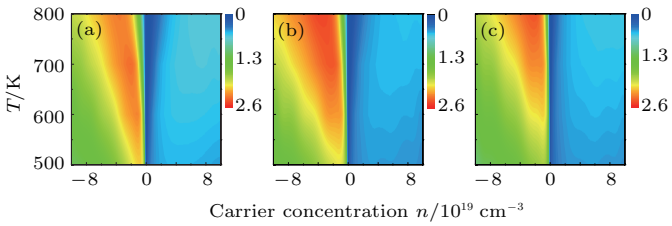


Fig. 6. (color online) Calculated zT map of $Mg_2Ge_xSn_{1-x}$ with (a) $x = 0.25$, (b) $x = 0.5$, and (c) $x = 0.75$ as a function of the carrier concentration n and the temperature T, respectively. The negative scale of the x axis stands for the n-type, while the positive scale represents the p-type.

4. Conclusion

In the present paper, the electronic structure and TE properties of solid solutions $Mg_2Ge_xSn_{1-x}$ ($x = 0.25$, 0.5, 0.75) have been studied by combining the first-principles calculations and the semi-classical Boltzmann theory. The special quasi-random structure method is used to produce the structures to model the solid solutions of $Mg_2Ge_xSn_{1-x}$. The maximum value of zT is predicted to be 2.45 for the n-type $Mg_2Ge_{0.5}Sn_{0.5}$ at 800 K with a carrier concentration of 3.28×10^{19} cm^{-3}, which is mainly due to the combination of high power factor and low lattice thermal conductivity. The zT values of solid solutions are higher than those of their corresponding pure compounds. The performance of the p-type $Mg_2Ge_xSn_{1-x}$ is inferior to the n-type one. The maximum zT value of 0.62 for the p-type appears in $Mg_2Ge_{0.25}Sn_{0.75}$ at 800 K with a carrier concentration of 8.66×10^{19} cm^{-3}. The n-type $Mg_2Ge_xSn_{1-x}$ solid solutions could be an outstanding TE material for practical applications due to its good TE performance. For p-type solid solutions, we still need to investigate other ways to enhance the TE performance in our future studies.

References

[1] Biswas K, He J Q, Blum I D, Wu C I, Hogan T P, Seidman D N, Dravid V P and Kanatzidis M G 2012 *Nature* **489** 414
[2] Zhao L D, Lo S H, Zhang Y S, Sun H, Tan G J, Uher C, Wolverton C, Dravid V P and Kanatzidis M G 2014 *Nature* **508** 373
[3] Zhao L D, Berardan D, Pei Y L, Byl C, Pinsard-Gaudart L and Dragoe N 2010 *Appl. Phys. Lett.* **97** 092118
[4] Barreteau C, Pan L, Amzallag E, Zhao L D, Berardan D and Dragoe N 2014 *Semicond. Sci. Technol.* **29** 64001
[5] Barreteau C, Pan L, Pei Y L, Zhao L D, Berardan D and Dragoe N 2013 *Funct. Mater. Lett.* **6** 1340007
[6] Rogl G, Grytsiv A, Rogl P, Peranio N, Bauer E, Zehetbauer M and Eibl O 2014 *Acta Mater.* **63** 30
[7] Sales B C, Mandrus D and Williams R K 1996 *Science* **272** 1325
[8] Sakurada S and Shutoh N 2005 *Appl. Phys. Lett.* **86** 82105
[9] Djaafri T, Djaafri A, Elias A, Murtaza G, Khenata R, Ahmed R and Rached D 2014 *Chin. Phys. B* **23** 087103
[10] Brown D R, Day T, Caillat T and Snyder G J 2013 *J. Electron. Mater.* **42** 2014
[11] Tan X, Shao H, Hu T, Liu G, Jiang J and Jiang H 2015 *Phys. Chem. Chem. Phys.* **17** 22872
[12] Zaitsev V K, Fedorov M I, Gurieva E A, Eremin I S, Konstantinov P P, Samunin A Y and Vedernikov M V 2006 *Phys. Rev. B* **74** 045207
[13] Liu W, Tan X J, Yin K, Liu H J, Tang X F, Shi J, Zhang Q J and Uher C 2012 *Phys. Rev. Lett.* **108** 166601
[14] Liu X H, Zhu T J, Wang H, Hu L P, Xie H H, Jiang G Y, Snyder G J and Zhao X B 2013 *Adv. Energy Mater.* **3** 1238
[15] Liu W, Tang X and Sharp J 2010 *J. Phys. D: Appl. Phys.* **43** 085406
[16] Khan A U, Vlachos N V, Hatzikraniotis E, Polymeris G S, Lioutas C B, Stefanaki E C, Paraskevopoulos K M, Giapintzakis I and Kyratsi T 2014 *Acta Mater.* **77** 43
[17] Gao P, Berkun I, Schmidt R, Luzenski M, Lu X, Bordon Sarac P, Case E and Hogan T 2013 *J. Electron. Mater.* **43** 1790
[18] Dasgupta T, Stiewe C, Boor J D and Müller E 2014 *Phys. Status Solidi* **211** 1250
[19] Sun J F and Singh D J 2016 *Phys. Rev. Appl.* **5** 024006
[20] Yang M J, Shen Q and Zhang L M 2011 *Chin. Phys. B* **20** 106202
[21] Busch G and Winkler U 1954 *Physica* **3** 1067
[22] Liu W, Kim H S, Chen S, Jie Q, Lv B, Yao M, Ren Z, Opeil C P, Wilson S, Chu C W and Ren Z 2015 *Proc. Natl. Acad. Sci. USA* **112** 3269
[23] Jiang G, Chen L, He J, Gao H, Du Z, Zhao X, Tritt T M and Zhu T 2013 *Intermetallics* **32** 312
[24] Boor J D, Saparamadu U, Mao J, Dahal K, Müller E and Ren Z 2016 *Acta Materialia* **120** 273
[25] Nakatsuji H 1979 *Chem. Phys. Lett.* **67** 329
[26] Zunger A, Wei S, Ferreira L G and Bernard J E 1990 *Phys. Rev. Lett.* **65** 353
[27] Souvatzis P, Katsnelson M I, Simak S, Ahuja R, Eriksson O and Mohn P 2004 *Phys. Rev. B* **70** 012201
[28] Doak J W, Wolverton C and Ozolins V 2015 *Phys. Rev. B* **92** 174306
[29] Kim J, Kwon H, Kim J H, Roh K M, Shin D and Jang H D 2015 *J. Alloys Compd.* **619** 788
[30] Xie Y P and Zhao S J 2011 *Comput. Mater. Sci.* **50** 2586
[31] Fedorov M I, Zaitsev V K, Eremin I S and Gurieva E A 2006 *Phys. Solid State* **48** 1486
[32] Zaitsev V K, Fedorov M I, Gurieva E A, Eremin I S, Konstantinov P P, Samunin A Y and Vedernikov M V 2005 *24th International conference on thermoelectrics, IEEE*, June 19–23, 2005, Clemson, USA, pp. 204–210
[33] Chakraborty M, Spitaler J, Puschnig P and Ambrosch-Draxl C 2010 *Comput. Phys. Commun.* **181** 913

[34] Kresse G and Furthmöller J 1999 *Phys. Rev. B* **54** 11169
[35] Blöchl P E 1994 *Phys. Rev. B* **50** 17953
[36] Perdew J P, Burke K and Ernzerhof M 1996 *Phys. Rev. Lett.* **77** 3865
[37] Monkhorst H J and Pack J D 1976 *Phys. Rev. B* **13** 5188
[38] Togo A and Tanaka I 2015 *Scr. Mater.* **108** 1
[39] Blaha P, Schwarz K, Madsen G, Kvasnicka D and Luitz J 2001 "WIEN2K", *An Augmented Plane Wave + Local Orbitals Program for Calculating Crystal Properties* (Schwarz K, Tech. Univ. Wien, Austria)
[40] Tran F and Blaha P 2009 *Phys. Rev. Lett.* **102** 226401
[41] Engel E and Vosko S H 1993 *Phys. Rev. B* **47** 13164
[42] Madsen G K H and Singh D J 2006 *Comput. Phys. Commun.* **175** 67
[43] Singh D J 2007 *Phys. Rev. B* **76** 085110
[44] Parker D and Singh D J 2011 *Phys. Rev. X* **1** 021005
[45] Parker D and Singh D J 2010 *Phys. Rev. B* **82** 035204
[46] Bader R F W 1985 *Acc. Chem. Res.* **18** 9
[47] Benhelal O, Chahed A, Laksari S, Abbar B, Bouhafs B and Aourag H 2005 *Phys. Status Solidi* **242** 2022
[48] Blanco A A, Francisco E and Luana V 2004 *Comput. Phys. Commun.* **158** 57
[49] Nye J F 1985 *Physical Properties of Crystals* (Oxford University Press)
[50] Luo D, Wang Y, Yan Y, Yang G and Yang J 2014 *J. Mater. Chem. A* **2** 15159
[51] Biswas K, He J, Zhang Q, Wang G, Uher C, Dravid V P and Kanatzidis M G 2011 *Nat. Chem.* **3** 160
[52] Snyder G J and Toberer E S 2008 *Nat. Mater.* **7** 105
[53] Jin Y R, Feng Z, Ye L, Yan Y and Wang Y 2016 *RSC Adv.* **6** 48728